Received: 27 December 2022 | Revised: 14 February 2023 | Accepted: 15 February 2023

DOI: 10.1002/alz.13034

Alzheimer's & Dementia®
THE JOURNAL OF THE ALZHEIMER'S ASSOCIATION

RESEARCH ARTICLE

Free water imaging of the cholinergic system in dementia with Lewy bodies and Alzheimer's disease

Julia Schumacher[1,2,3] | Nicola J. Ray[4] | Calum A. Hamilton[1] | Maurizio Bergamino[5] | Paul C. Donaghy[1] | Michael Firbank[1] | Rosie Watson[6,7] | Gemma Roberts[1] | Louise Allan[1,8] | Nicola Barnett[1] | John T. O'Brien[9] | Alan J. Thomas[1] | John-Paul Taylor[1]

[1]Translational and Clinical Research Institute, Faculty of Medical Sciences, Newcastle University, Campus for Ageing and Vitality, Newcastle upon Tyne, Nebraska4 5PL, UK

[2]Department of Neurology, University Medical Center Rostock, Rostock, Germany

[3]German Center for Neurodegenerative Diseases (DZNE) Rostock-Greifswald, Rostock, Germany

[4]Health, Psychology and Communities Research Centre, Department of Psychology, Manchester Metropolitan University, Manchester, UK

[5]Barrow Neurological Institute, Neuroimaging Research, Phoenix, Arizona, USA

[6]Department of Medicine, The Royal Melbourne Hospital, The University of Melbourne, Parkville, VIC, Australia

[7]Population Health and Immunity Division, The Walter and Eliza Hall Institute of Medical Research, Parkville, Australia

[8]University of Exeter Medical School, Exeter, UK

[9]Department of Psychiatry, University of Cambridge School of Medicine, Cambridge, UK

Correspondence
Julia Schumacher, German Center for Neurodegenerative Diseases (DZNE), Gehlsheimer Str. 20, 18147 Rostock, Germany.
Email: julia.schumacher@dzne.de

Abstract

INTRODUCTION: Degeneration of cortical cholinergic projections from the nucleus basalis of Meynert (NBM) is characteristic of dementia with Lewy bodies (DLB) and Alzheimer's disease (AD), whereas involvement of cholinergic projections from the pedunculopontine nucleus (PPN) to the thalamus is less clear.

METHODS: We studied both cholinergic projection systems using a free water-corrected diffusion tensor imaging (DTI) model in the following cases: 46 AD, 48 DLB, 35 mild cognitive impairment (MCI) with AD, 38 MCI with Lewy bodies, and 71 controls.

RESULTS: Free water in the NBM-cortical pathway was increased in both dementia and MCI groups compared to controls and associated with cognition. Free water along the PPN-thalamus tract was increased only in DLB and related to visual hallucinations. Results were largely replicated in an independent cohort.

DISCUSSION: While NBM-cortical projections degenerate early in AD and DLB, the thalamic cholinergic input from the PPN appears to be more selectively affected in DLB and might associate with visual hallucinations.

KEYWORDS
free water-corrected diffusion tensor imaging, mild cognitive impairment, nucleus basalis of Meynert, pedunculopontine nucleus, visual hallucinations

Highlights

- Free water in the NBM-cortical cholinergic pathways is increased in AD and DLB.
- NBM-cortical pathway integrity is related to overall cognitive performance.
- Free water in the PPN-thalamus cholinergic pathway is only increased in DLB, not AD.
- PPN-thalamus pathway integrity might be related to visual hallucinations in DLB.

1 | BACKGROUND

Dementia with Lewy bodies (DLB) and Alzheimer's disease (AD) are both characterized by cholinergic deficits.[1] There are two major sources of cholinergic projections in the brain. The first, the nucleus basalis of Meynert (NBM) in the basal forebrain, is predominantly composed of cholinergic neurons, has widespread connections to the entire cortex, and therefore is the main source of cortical cholinergic input.[2] This has been widely investigated in AD and DLB, and early degeneration of the NBM and its cortical projections has been found in both conditions.[3–5]

The second, the pedunculopontine nucleus (PPN) in the brainstem, contains cholinergic neurons and connects with the basal ganglia, thalamus, and lower brainstem and spinal cord.[6,7] It is implicated in motor function, and its decline in Parkinson's disease (PD)[8] and also plays a role in cognition.[9] It provides the main source of cholinergic innervation to the thalamus,[10,11] thereby influencing thalamocortical activity.[12] *Post-mortem* studies have found degeneration of the PPN in DLB[13,14] and an association between PPN neuronal loss and the presence of visual hallucinations in PD.[15,16] Furthermore, previous positron emission tomography (PET) and *post-mortem* studies have found cholinergic denervation within the thalamus in DLB and have speculated that this might be due to loss of cholinergic input from the PPN.[17,18] However, no study has directly investigated these pathways in DLB yet, and in general the PPN has been much less widely studied than the NBM.

One reason for the scarcity of in vivo studies of the PPN is its location in the brainstem, which precludes a volumetric analysis using T1-weighted magnetic resonance imaging (MRI). More recently, diffusion-weighted imaging data have been successfully used to characterize the microstructural properties of deep gray matter (GM) structures such as the PPN.[19,20] In contrast to widely used diffusion tensor imaging (DTI) models that fit a single tensor in each voxel, a bi-tensor model allows for the estimation of the fractional volume of free water within each voxel.[21] This measure describes water molecules whose diffusion is not restricted by cellular structures and is thought to mainly represent the extracellular space[21] and be related to neuroinflammation.[22,23]

There may be heterogeneous degeneration in the NBM and PPN that contributes differently to the symptoms of DLB and AD, but no studies have assessed these two key components of the cholinergic system in the same participants in vivo. In this study, we therefore sought to investigate both nuclei and their projections to the cortex and the thalamus, respectively, using a free water-corrected DTI model. We studied these pathways across the disease spectrum by including people with mild cognitive impairment (MCI) as well as people with more advanced disease to understand better how microstructural changes in different parts of the cholinergic system relate to different aspects of cognitive function and whether they are predictive of longitudinal changes in cognition. For the NBM, we analyzed the two main cortical pathways, which were described in previous studies.[5,24] For the PPN, based on the aforementioned evidence from previous studies, we focused on its thalamic projections and were specifically interested in how the integrity of this pathway might relate to visual hallucinations in DLB.

RESEARCH IN CONTEXT

1. **Systematic review**: The authors reviewed the literature using traditional sources (e.g. PubMed). While the nucleus basalis of Meynert (NBM) has been widely studied in both Alzheimer's disease (AD) and dementia with Lewy bodies (DLB), we found no previous in vivo study of the pedunculopontine nucleus (PPN) or the integrity of the PPN-thalamus cholinergic pathways in DLB or AD.
2. **Interpretation**: While confirming previous findings of an early and non-specific degeneration of NBM-cortical cholinergic projections in both AD and DLB, our study reveals that the PPN-thalamus cholinergic projection system is more differentially affected in DLB and appears to be relatively spared in AD.
3. **Future directions**: While degeneration of NBM pathways occurs early, we found changes in the PPN-thalamus pathway only at the dementia stage in DLB, suggesting that these might occur later on in the disease course. Longitudinal imaging studies with more advanced multishell acquisitions are needed to confirm this cross-sectional observation.

2 | METHODS

2.1 | Participants

This study included two independent cohorts (Cohort 1 for the main analysis and Cohort 2 as a validation dataset). All participants were over 60 years of age. Patients were recruited from the local community-dwelling population who had been referred to old-age psychiatry/neurology services.[4,5,25,26] Control participants were recruited from a local research register and from relatives/friends of patients and had no history of psychiatric/neurological illness. Diagnoses were performed independently by a consensus panel of three experienced clinicians in accordance with consensus clinical criteria. Cohort 1 included 48 patients with probable DLB,[27] 46 with probable AD,[28] 38 with probable MCI with Lewy bodies (MCI-LB),[29] 35 with MCI due to Alzheimer's disease (MCI-AD),[30] and 71 cognitively unimpaired controls. Cohort 2 included 34 AD, 34 DLB, 35 controls, and no MCI participants.

All participants underwent a clinical assessment including Mini-Mental State Examination (MMSE), Unified Parkinson's Disease Rating

Scale (UPDRS) part III, Neuropsychiatric Inventory (NPI), and Clinician Assessment of Fluctuations (CAF). Participants also performed computerized tests, including a choice reaction time task and a test of phonemic fluency (combined number of words produced in three 60-s blocks beginning with the letters F, A, and S).

All participants had baseline imaging data and clinical assessments. The MCI participants were followed up annually and re-assessed with neuropsychological testing and clinical panel review of diagnosis.[31] Additionally, a subset of dementia and control participants from Cohort 1 (21 DLB, 15 AD, and 48 controls) and Cohort 2 (14 DLB, 24 AD, and 32 controls) underwent a follow-up examination after 12 months.[25]

Studies were approved by Newcastle & North Tyneside 1 and 2 Research Ethics Committee (10/H0906/19, 15/NE/0420 and 13/NE/0064), and written informed consent was obtained from all participants.

2.2 | MRI acquisition/preprocessing

Cohort 1: T1-weighted magnetic resonance images were acquired on a 3 T Philips Intera Achieva scanner with magnetization prepared rapid gradient echo (MPRAGE) sequence, sagittal acquisition, echo time (TE) = 4.6 ms, repetition time (TR) = 8.3 ms, inversion time = 1250 ms, flip angle = 8°, SENSE factor = 2, in-plane field of view 240 × 240 mm^2 with slice thickness 1.0 mm, yielding a voxel size of 1.0 × 1.0 × 1.0 mm^3. Diffusion-weighted images (DWI) were acquired with TR = 6126 ms, TE = 70 ms, 124×120 matrix, 270×270 field of view, 59 slices, slice thickness 2.11 mm, 64 gradient orientations (b = 1000 s/mm^2), and six images without diffusion weighting (b = 0 s/mm^2, b0).

Cohort 2: T1-weighted MR and diffusion-weighted images were acquired on the same 3T Philips Intera Achieva scanner. T1-weighted data: 3D MPRAGE, sagittal acquisition, 1 mm isotropic resolution, 240 × 240 × 180 matrix, TR = 9.6 ms, TE = 4.6 ms; flip angle = 8°, SENSE factor = 2. DWI data: TR = 2524 ms, TE = 71 ms, 128 × 128 matrix, 24 slices, 6 mm slice thickness, 2 mm in-plane resolution, 16 diffusion directions with b = 1000 s/mm^2, and one b0 scan.

All DWI data were visually inspected for artifacts and processed using FSL (version 6.0.2): (1) Brain extraction with FSL's bet function and (2) FSL's eddy tool to correct for eddy currents and head motion.[5]

2.3 | Regions of interest

The NBM mask (Figure 1A) was based on the Ch4 region of a cytoarchitectonic map of the cholinergic basal forebrain in MNI T1 space that had been derived from combined histology and MRI of a *post-mortem* brain.[32]

For the PPN, we used a stereotactic map that had been derived from combined histology and *post-mortem* MRI of the brain of a 66-year-old woman who showed no signs of Parkinsonism or cognitive decline[19] (Figure 2A).

2.4 | Tractography

FSL's BedpostX was applied to the eddy-corrected DWI data to calculate the diffusion parameters using a standard ball-and-sticks model with three fibers modeled per voxel. Probabilistic tracking was performed using FSL's ProbtrackX by generating 5000 random samples from the respective seed regions of interest (ROIs) (NBM/PPN).

The NBM tractography analysis used ROIs of the cingulum and external capsule (obtained from the Johns Hopkins University white matter atlas in FSL) as waypoint masks to constrain the tractography to the lateral and medial NBM pathways identified in previous studies[5,24] and ROIs of the anterior commissure (obtained from FSL's XTRACT tool) and brainstem (estimated using FSL's FIRST segmentation routine) as exclusion masks to avoid contamination of estimated tracts from non-cholinergic pathways[2,24] (see Schumacher et al.[5] for details).

To identify tracts connecting the PPN and the thalamus, we used a thalamus ROI as target mask (from FSL's Harvard-Oxford Subcortical Atlas), thereby only retaining tracts that end in the thalamus. Exclusion ROIs for the PPN-thalamus tractography included inferior, middle, and superior cerebellar peduncle (from Johns Hopkins University WM atlas) and caudate, putamen, and pallidum (from Harvard-Oxford Atlas) to avoid pathways from the PPN toward lower brainstem nuclei, down to the spinal cord, and to the basal ganglia. Before the tractography was run, all ROIs were transformed into individual T2 space using Advanced Normalization Tools' (ANTs) non-linear SyN algorithm.

An unbiased group template was created with ANTs' buildtemplate function using b0 images of 100 randomly selected participants (20 from each group), and the non-thresholded probtrackX tracts were transformed from individual T2 space to this group template space. Medial and lateral NBM group tracts were created by selecting all voxels that were included in at least 50% of the individual tracts.[5] The threshold for the PPN-thalamus pathway was set at 70%. These thresholds were based on visual inspection of the resulting tracts. Group tracts were then transformed back into each participant's T2 space.

The tractography was only performed in Cohort 1. The resolution and number of diffusion directions in Cohort 2 does not allow for accurate tractography with ProbtrackX. Therefore, for the analysis in Cohort 2, the estimated tracts from Cohort 1 were used as templates and transformed into each participant's T2 space for further analysis.

2.5 | Extraction of diffusivity metrics

A bi-tensor model was fit to the eddy-corrected diffusion data using custom MATLAB scripts to estimate free water fraction (FWf) and free water-corrected mean diffusivity (cMD) and axial diffusivity (cAxD) within each voxel.[21]

FWf, cMD, and cAxD were extracted from the NBM and the PPN. To ensure that these were constrained to GM, the NBM was masked with the GM mask estimated from the segmentation of T1-weighted images.[5] For the PPN, which has WM pathways from the brainstem running through it, the analysis was restricted to voxels with fractional

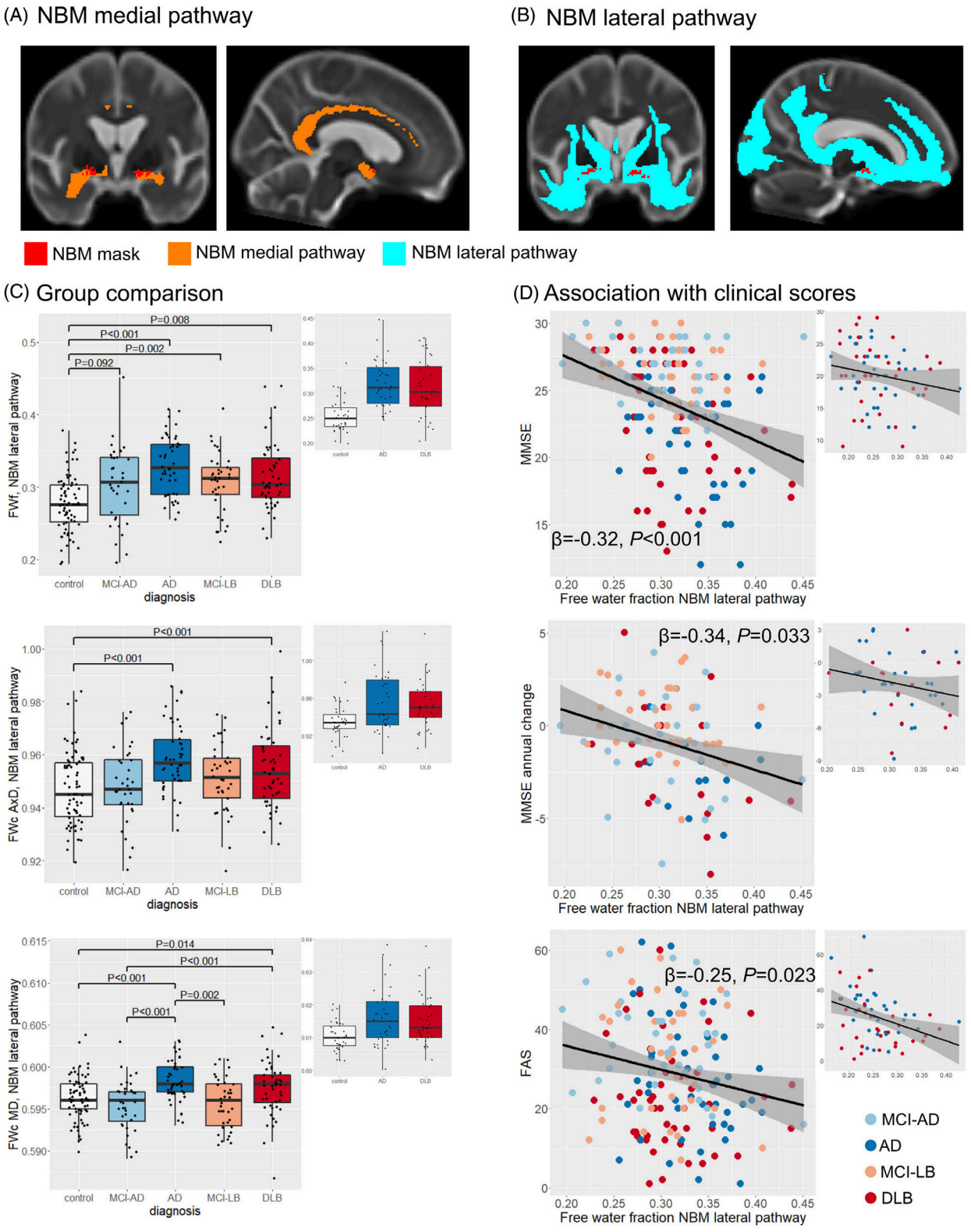

FIGURE 1 Analysis of NBM pathways. (A) NBM medial and (B) NBM lateral pathway as identified in Schumacher et al. (2022)[5], overlaid on the unbiased group template used in the tractography analysis. (C) Group comparison of free water fraction and diffusivity metrics for NBM pathways (Table 2). In each box plot the central line corresponds to the sample median, the upper and lower borders of the box represent the 25th and 75th percentiles, respectively, and the length of the whiskers corresponds to 1.5 times the interquartile range. (D) Association between free water fraction and clinical scores (Table 4). The main plots show results from Cohort 1, and the small plots show results in Cohort 2 as a validation cohort. AD, Alzheimer's disease; AxD, axial diffusivity; DLB, dementia with Lewy bodies; FAS, phonemic fluency test; FWc, free water-corrected; FWf, free water fraction; MCI-AD, mild cognitive impairment due to Alzheimer's disease; MCI-LB, MCI with Lewy bodies; MD, mean diffusivity; MMSE, Mini-Mental State Examination; NBM, nucleus basalis of Meynert.

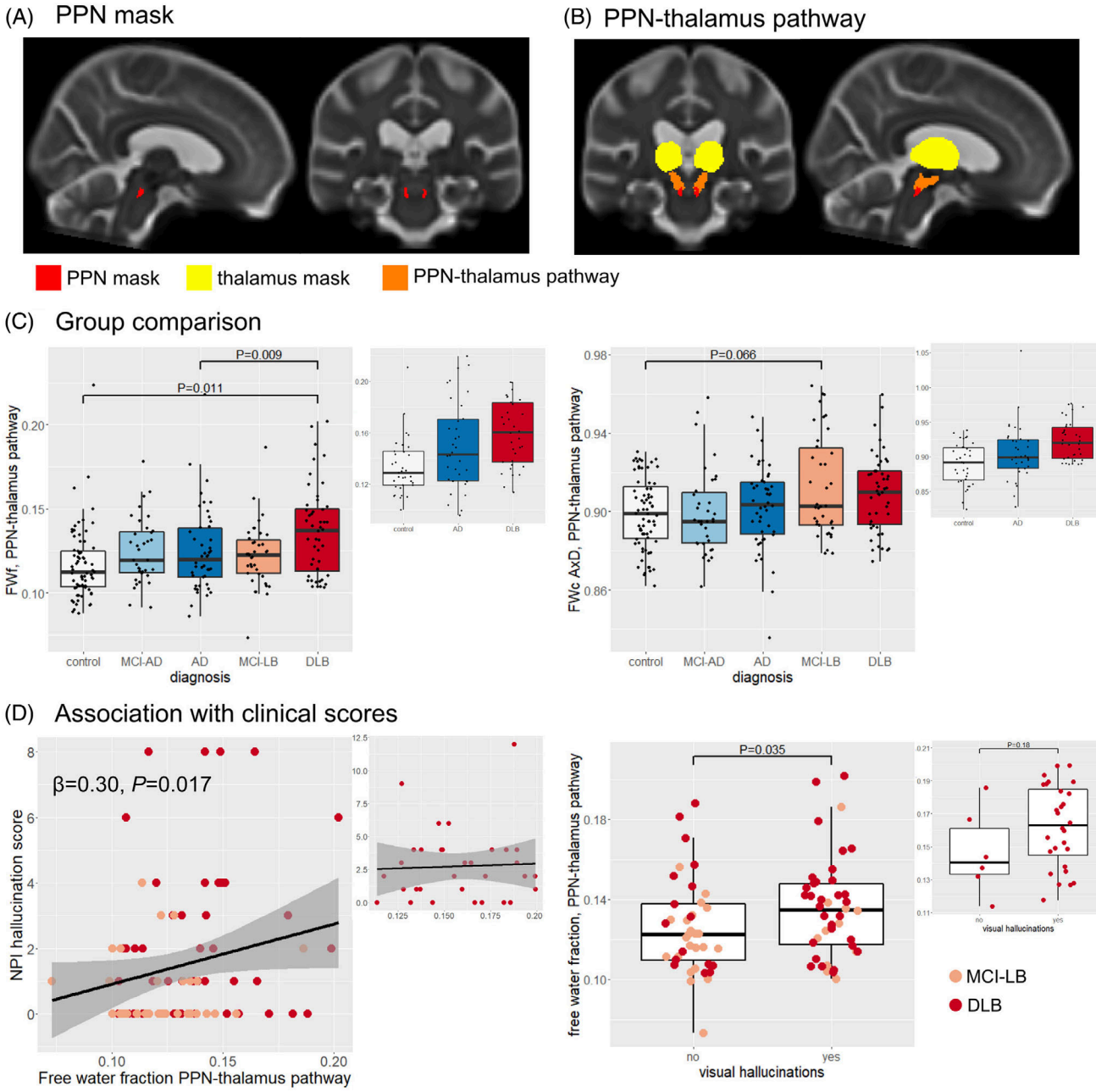

FIGURE 2 Analysis of PPN-thalamus pathway. (A) PPN mask. (B) Pathway from PPN to thalamus. (C) Group comparison of free water fraction and axial diffusivity in PPN-thalamus pathway (Table 3). In each box plot the central line corresponds to the sample median, the upper and lower borders of the box represent the 25th and 75th percentiles, respectively, and the length of the whiskers corresponds to 1.5 times the interquartile range. (D) Association between free water fraction and NPI hallucination score in Lewy body groups (Table 4). The main plots show results from Cohort 1, and the small plots show results in Cohort 2 as a validation cohort. AD, Alzheimer's disease; AxD, axial diffusivity; DLB, dementia with Lewy bodies; FWc, free water-corrected; FWf, free water fraction; MCI-AD, mild cognitive impairment due to Alzheimer's disease; MCI-LB, MCI with Lewy bodies; MD, mean diffusivity; MMSE, Mini-Mental State Examination; NBM, nucleus basalis of Meynert; NPI, Neuropsychiatric Inventory; PPN, pedunculopontine nucleus.

anisotropy < 0.77 based on values reported in Alho et al.[19] (mean+1 standard deviation). Furthermore, FWf, cMD, and cAxD were extracted from each of the estimated WM pathways (medial and lateral NBM tract and PPN-thalamus tract).

To test the specificity of any effects for the cholinergic pathways, we created WM control masks by subtracting the estimated tracts from a whole-brain WM mask (from running FSL FAST on each participant's T1-weighted image). For the analysis of diffusivity metrics in NBM and PPN, GM control masks were created by subtracting the respective ROIs from a whole-brain GM mask. We included these covariates to specifically investigate differences in the cholinergic pathways that go beyond more general neurodegenerative processes that would be

TABLE 1 Demographics and clinical information at baseline.

	Controls	MCI-AD	MCI-LB	AD	DLB	Group differences
Cohort 1						
N	71	35	38	46	48	
N with follow-up	48	29	35	15	21	
Time to follow-up (in days)	382.0 (336-493)	481.1 (363-783)	405.0 (358-832)	378.9 (350-483)	382.3 (350-560)	$F(4,142) = 9.2$, $P < .001$ P(HC,MCI-AD) < 0.001 P(MCI-AD, MCI LB) = 0.001 P(MCI-AD,AD) < 0.001 P(MCI-AD,DLB) < 0.001
Male: female	51:20	15:20	34:4	38:8	35:13	$\chi^2 = 23.4$, $P < .001$[a] P(HC,MCI-AD) = 0.004 P(HC,MCI-LB) = 0.034 P(MCI-AD,MCI LB) < 0.001 P(MCI-AD,AD) < 0.001 P(MCI-AD,DLB) = 0.006
Age	75.3 (6.9)	75.8 (7.8)	74.5 (6.5)	77.1 (7.5)	76.2 (6.6)	$F(4,233) = 0.83$, $P = .51$[b]
AChEI	–	7 (21%)[e]	18 (49%)[f]	39 (85%)	44 (92%)	$\chi^2 = 55.7$, $P < .001$[c] P(MCI-AD, MCI-LB) = 0.02 P(MCI-AD,AD) < 0.001 P(MCI-AD,DLB) < 0.001 P(MCI-LB,AD) < 0.001 P(MCI-LB,DLB) < 0.001
PD meds	–	0e	4 (11%)[f]	0	21 (44%)	P(MCI-LB,DLB) = 0.001
MMSE	28.8 (1.0)	26.8 (2.1)[g]	26.4 (2.4)	21.1 (4.0)	22.6 (4.5)	$F(3,163) = 26.0$, $P < .001$[d] P(MCI-AD,AD) < 0.001 P(MCI-AD,DLB) < 0.001 P(MCI-LB,AD) < 0.001 P(MCI-LB,DLB) < 0.001
UPDRS III motor scale	–	8.3 (7.3)	12.3 (7.6)	3.6 (2.7)	19.4 (8.8)	$F(3,162) = 42.3$, $P < 0.001$[d] P(MCI-AD,AD) = 0.02 p(MCI-AD,DLB) < 0.001 P(MCI-LB,AD) < 0.001 P(MCI-LB,DLB) < 0.001 P(AD,DLB) < 0.001
CAF total	–	1.4 (2.7)[h]	3.7 (4.3)[i]	1.9 (3.9)[k]	5.0 (4.4)[l]	$F(3,150) = 6.7$, $P < .001$[d] P(MCI-AD,DLB) = 0.002 P(AD,DLB) = 0.002
NPI total	–	8.4 (9.5)[h]	16.0 (13.0)[i]	8.5 (8.7)[k]	14.3 (13.4)[l]	$F(3,150) = 4.3$, $P = .006$[d] P(MCI-LB,AD) = 0.03
NPI hall	–	0.04 (0.2)[m]	0.6 (1.1)[i]	0.07 (0.4)[k]	2.1 (2.4)[l]	$F(3,148) = 18.5$, $P < .001$[d] P(MCI-AD,DLB) < 0.001 P(AD,DLB) < 0.001 P(MCI-LB,DLB) < 0.001
Cohort 2						
N	35	–	–	34	34	
N with follow-up	32	–	–	24	14	
Time to follow-up (in days)	372.5 (340-412)	–	–	378.7 (354-427)	381.5 (357-434)	$F(2,67) = 1.9$, $P = .16$[b]
Male: female	20:15	–	–	19:15	27:7	$\chi^2 = 5.2$, $P = .07$[a]
Age	76.7 (5.2)	–	–	78.2 (5.7)	78.2 (7.0)	$F(2,100) = 0.7$, $P = .51$[b]
AChEI	–	–	–	31 (91%)	29 (85%)	$\chi^2 = 0.1$, $P = .71$[c]
PD meds	–	–	–	0	11 (32%)	–

(Continues)

TABLE 1 (Continued)

	Controls	MCI-AD	MCI-LB	AD	DLB	Group differences
MMSE	29.1 (1.0)	–	–	19.9 (4.1)	20.4 (5.3)	t62 = 0.4, $P = .69$[d]
UPDRS III motor scale	–	–	–	5.6 (4.4)	25.6 (10.6)	t44 = 10.8, $P < .001$[d]
CAF total	-	–	–	1.9 (3.3)[e]	6.2 (3.8)[n]	t61 = 4.8, $P < .001$[d]
NPI total	–	–	–	16.3 (11.9)[e]	21.9 (17.2)[n]	t55 = 1.5, $P = .13$[d]
NPI hall	–	–	–	0.24 (0.79)[e]	2.8 (2.7)[n]	t36 = 5.0, $P < .001$[d]

Note: Mean (standard deviation). More information on the subset of participants with follow-up data can be found in Supplementary Tables S1 and S2.
Abbreviations: AChEI, number of patients taking acetylcholinesterase inhibitors; AD, Alzheimer's disease; CAF total, Clinician Assessment of Fluctuation total score; DLB, dementia with Lewy bodies; HC, healthy controls; MCI-AD, mild cognitive impairment with Alzheimer's disease; MCI-LB, probable mild cognitive impairment with Lewy bodies; MMSE, Mini-Mental State Examination; NPI, Neuropsychiatric Inventory; NPI hall, NPI hallucination score; PD meds, number of patients taking dopaminergic medication for the management of Parkinson's disease symptoms; UPDRS III, Unified Parkinson's Disease Rating Scale III (motor subsection).
[a]Chi-square test all groups.
[b]Univariate ANOVA all groups.
[c]Chi-square test patient groups.
[d]Univariate ANOVA patient groups.
[e]$n = 33$. [f]$n = 37$. [g]$n = 34$. [h]$n = 27$. [i]$n = 35$. [k]$n = 45$. [l]$n = 47$. [m]$n = 25$. [n]$n = 32$.

expected in the clinical groups. However, as a comparison we also provide results without including these covariates in the supplementary material.

2.6 | Statistics

All statistical analyses were performed in R (https://www.r-project.org/), separately in the two cohorts. FWf, cMD, and cAxD within the NBM, PPN, NBM medial and lateral pathways, and the PPN-thalamus pathway were compared between groups using univariate analysis of covariance (ANCOVA) controlling for age, sex, and diffusivity metrics from the respective WM/GM control mask, followed by Bonferroni-corrected post hoc tests.

To test the combinative effect of changes in the different cholinergic pathways on clinical scores, a multiple linear regression model was run across all MCI and dementia patients with the clinical score as dependent variable and FWf from the lateral NBM and the PPN-thalamus pathway as predictor variables, controlling for age, sex, diagnosis, and FWf from the WM control mask. Associations with DLB-specific symptoms (CAF, NPI hallucination subscale, and UPDRS) were calculated only in the MCI-LB and DLB patients. To assess whether baseline FWf was related to changes in cognition, we calculated annual change scores by subtracting the cognitive score at baseline from the follow-up score, divided by the time between baseline and follow-up in years. A similar regression model was then run with annual change scores as dependent variable, including baseline scores as additional covariates.

To test the influence of cholinesterase inhibitors, we compared patients taking cholinesterase inhibitors ($n = 108$) with patients not taking these medications ($n = 56$) using univariate ANCOVAs controlling for cognitive status (MCI/dementia) since more dementia than MCI patients were taking cholinesterase inhibitors.

The interrelationship between the different NBM and PPN measures was assessed by partial correlations across all groups and in each group separately, controlling for FWf from remaining WM/GM.

3 | RESULTS

3.1 | Demographics

Table 1 shows demographic and clinical information for both cohorts (see Supplementary Table S1 and Supplementary Table S2 for the subset with follow-up data). Time between baseline and follow-up was significantly longer in the MCI-AD patients due to delays in scheduling follow-ups caused by the Covid-19 pandemic. Therefore, we accounted for time between baseline and follow-up when calculating cognitive change scores.

3.2 | Group comparison of NBM and NBM tracts

FWf within the NBM was increased in AD and DLB compared to controls with no significant changes in the MCI groups (Table 2A) in Cohort 1; however, no significant group differences were found in Cohort 2.

FWf within the medial NBM tract (Figure 1A), though it was increased in DLB and AD compared to controls, was not significantly different between the groups in Cohort 1, but the increase was significant in Cohort 2 (Table 2B). cMD and cAxD along this pathway were increased in AD and DLB compared to the control and MCI groups in Cohort 1, and the increase in DLB was replicated in Cohort 2.

In the NBM lateral pathway (Figure 1B), FWf was increased in both MCI and dementia groups compared to controls (although only marginally significant in the MCI-AD group). cMD and cAxD in the NBM lateral pathway were increased in AD and DLB compared to con-

TABLE 2 Mean (standard deviation) and group comparison of diffusivity metrics from NBM and the two NBM pathways.

			Controls	MCI-AD	MCI-LB	AD	DLB	Group differences	
A) NBM	FWf	Cohort 1	0.39 (0.07)	0.43 (0.07)	0.41 (0.06)	0.47 (0.07)	0.45 (0.07)	$F(4,230) = 4.1$, $P = .003$ P(HC,AD) = 0.003 P(HC,DLB) = 0.049	HC < AD, DLB
		Cohort 2	0.48 (0.09)	–	–	0.56 (0.14)	0.52 (0.13)	$F(2,97) = 1.53$, $P = .22$	
	FWc-AxD	Cohort 1	0.92 (0.06)	0.90 (0.06)	0.88 (0.05)	0.93 (0.06)	0.93 (0.06)	$F(4,230) = 3.2$, $P = .02$ P(HC,MCI-LB) = 0.02	HC > MCI-LB
		Cohort 2	1.007 (0.164)	–	–	1.004 (0.178)	0.973 (0.153)	$F(2,97) = 0.19$, $P = .83$	
	FWc-MD	Cohort 1	0.593 (0.02)	0.585 (0.02)	0.588 (0.02)	0.588 (0.01)	0.592 (0.02)	$F(4,230) = 1.4$, $P = .23$	
		Cohort 2	0.648 (0.066)	–	–	0.661 (0.093)	0.658 (0.088)	$F(2,97) = 0.37$, $P = .69$	
B) NBM medial pathway	FWf	Cohort 1	0.22 (0.04)	0.24 (0.05)	0.23 (0.04)	0.26 (0.04)	0.25 (0.04)	$F(4,230) = 1.8$, $P = .12$	
		Cohort 2	0.22 (0.03)	–	–	0.26 (0.05)	0.26 (0.06)	$F(2,97) = 7.66$, $P < .001$ P(HC,AD) = 0.003, P(HC,DLB) = 0.003	HC < AD, DLB
	FWc-AxD	Cohort 1	1.04 (0.02)	1.04 (0.03)	1.05 (0.02)	1.05 (0.03)	1.05 (0.03)	$F(4,230) = 7.1$, $P < .001$ P(HC,AD) < 0.001 P(HC,DLB) < 0.001 P(MCI-AD,AD) = 0.04 P(MCI-AD,DLB) = 0.06	HC, MCI-AD < AD, DLB
		Cohort 2	0.973 (0.035)	–	–	1.0 (0.065)	1.007 (0.057)	$F(2,97) = 3.38$, $P = .038$ P(HC,AD) = 0.18, P(HC,DLB) = 0.045	HC < DLB
	FWc-MD	Cohort 1	0.598 (0.003)	0.597 (0.003)	0.598 (0.003)	0.601 (0.004)	0.600 (0.004)	$F(4,230) = 7.7$, $P < .001$ P(HC,AD) < 0.001 P(HC,DLB) = 0.009 P(MCI-AD,AD) < 0.001 P(MCI-AD,DLB) = 0.01 P(MCI-LB,AD) = 0.008	HC, MCI-AD, MCI-LB < AD, DLB
		Cohort 2	0.604 (0.005)	–	–	0.61 (0.012)	0.612 (0.017)	$F(2,97) = 3.97$, $P = .022$ P(HC,AD) = 0.22, P(HC,DLB) = 0.020	HC < DLB

(Continues)

TABLE 2 (Continued)

			Controls	MCI-AD	MCI-LB	AD	DLB	Group differences	
C) NBM lateral pathway	FWf	Cohort 1	0.28 (0.04)	0.30 (0.05)	0.31 (0.04)	0.33 (0.04)	0.31 (0.05)	$F(4,230) = 7.8$, $P < .001$ P(HC,MCI-AD) = 0.09 P(HC, MCI-LB) = 0.002 P(HC,AD) < 0.001 P(HC,DLB) = 0.008	HC < MCI-AD, MCI-LB, AD, DLB
		Cohort 2	0.26 (0.03)	–	–	0.32 (0.05)	0.31 (0.06)	$F(2,97) = 16.75$, $P < .001$ P(HC,AD) < 0.001, P(HC,DLB) < 0.001	HC < AD, DLB
	FWc-AxD	Cohort 1	0.947 (0.01)	0.948 (0.01)	0.951 (0.01)	0.959 (0.01)	0.955 (0.02)	$F(4,230) = 11.3$, $P < .001$ P(HC,AD) < 0.001 P(HC,DLB) = 0.001 P(MCI-AD,AD) < 0.001 P(MCI-AD,DLB) = 0.01 P(MCI-LB,AD) < 0.001	HC, MCI-AD, MCI-LB < AD, DLB
		Cohort 2	0.935 (0.017)	–	–	0.956 (0.031)	0.952 (0.025)	$F(2,97) = 6.46$, $P = .002$ P(HC,AD) = 0.003, P(HC,DLB) = 0.033	HC < AD, DLB
	FWc-MD	Cohort 1	0.596 (0.002)	0.595 (0.003)	0.596 (0.003)	0.598 (0.002)	0.598 (0.003)	$F(4,230) = 11.8$, $P < .001$ P(HC,AD) < 0.001 P(HC,DLB) = 0.01 P(MCI-AD,AD) < 0.001 P(MCI-AD,DLB) < 0.001 P(MCI-LB,AD) = 0.002	HC, MCI-AD, MCI-LB < AD, DLB
		Cohort 2	0.61 (0.004)	–	–	0.616 (0.009)	0.615 (0.008)	$F(2,97) = 5.72$, $P = .004$ P(HC,AD) = 0.006, P(HC,DLB) = 0.035	HC < AD, DLB

Note: Groups were compared by ANCOVAs including covariates for age, sex, and diffusivity metrics from a control mask. *P*-values from post hoc tests are Bonferroni-corrected for multiple comparisons. Axial and mean diffusivity values are multiplied by 1000.

All *P*-values from post hoc comparisons that are not shown are >0.05.

Abbreviations: AD, Alzheimer's disease; DLB, dementia with Lewy bodies; FWc-AxD, free water-corrected axial diffusivity; FWc-MD, free water-corrected mean diffusivity; FWf, free water fraction; HC, healthy controls; MCI-AD, mild cognitive impairment due to Alzheimer's disease; MCI-LB, MCI with Lewy bodies; NBM, nucleus basalis of Meynert.

trols and MCI (Figure 1C, Table 2C). All results for the NBM lateral pathway were replicated in Cohort 2.

For comparison, results from a standard single-tensor DTI model (i.e. without considering free water) can be found in Supplementary Table S3, and statistical results without controlling for whole-brain metrics are presented in Supplementary Table S4.

3.3 | Group comparison of PPN and PPN-thalamus tract

Within the PPN itself (Figure 2A), there were no significant group differences in either cohort (Table 3A).

FWf along the PPN-thalamus tract (Figure 2B) was significantly increased in DLB compared to controls and AD (Table 3B, Figure 2C). The increase in DLB compared to controls was also evident in Cohort 2. cAxD was slightly increased in the Lewy body groups compared to controls in both cohorts.

Results from the single-tensor DTI model can be found in Supplementary Table S5 and results without controlling for whole-brain metrics in Supplementary Table S6.

3.4 | Association with clinical symptoms

Increased FWf in the NBM lateral pathway was associated with lower MMSE scores and worse performance on phonemic fluency tests at baseline, as well as with a greater longitudinal decline in those scores (Table 4, Figure 1D) and with performance on a choice reaction time task, similarly in both cohorts. There also appeared to be an association with CAF scores in the Lewy body groups; however, this disappeared if age was not included as a covariate.

Increased FWf in the PPN-thalamus pathway was associated with higher hallucination scores in the Lewy body groups (Table 4, Figure 2D, $\beta = 0.3$, $p = .017$), however only in Cohort 1. When FWf in the PPN itself was also included in the regression analysis, the association between FWf in the PPN-thalamus pathway and visual hallucination scores was even stronger ($\beta = 0.39$, $p = .006$), while FWf in the PPN was not related to hallucination scores ($\beta = -0.18$, $p = .16$). This finding was followed up by an ANCOVA comparing FWf in the PPN-thalamus pathway between those patients who had visual hallucinations ($N = 42$ and $N = 28$ in Cohorts 1 and 2, respectively) versus those who did not ($N = 40$ and $N = 6$ in Cohorts 1 and 2, respectively) controlling for age, sex, and FWf from the WM control mask. This showed that FWf in the PPN-thalamus tract was significantly increased in those with visual hallucinations in Cohort 1 ($p = .035$, Figure 2D) with a similar tendency in Cohort 2, although this was not significant ($p = .18$).

Regression results from the single-tensor DTI model are presented in Supplementary Table S7 and regressions without controlling for whole-brain metrics in Supplementary Table S8.

Patients who were taking cholinesterase inhibitors showed a slight but significant increase in cAxD compared to patients not on these agents ($p = .04$), but apart from that there were no significant differences between patients based on cholinesterase inhibitor use (Supplementary Table S9).

3.5 | Association between NBM and PPN measures

Supplementary Figure S1 shows the correlation structure between FWf within the NBM, the PPN, and the estimated WM tracts. While the correlation between the two NBM tracts was high in all groups, the different NBM and PPN measures only showed low to medium correlations.

4 | DISCUSSION

In this study, we investigated the integrity of the two main cholinergic projection systems in DLB and AD and their differential association with cognition and disease progression using free water imaging. Our findings suggest that the NBM-cortical projections are similarly affected early in both conditions and are related to different cognitive functions. In contrast, the PPN-thalamus system was more specifically affected in DLB and appeared relatively spared in AD, and these changes might be related to symptoms that are more specific to Lewy body disease. These results were largely replicated in an independent dataset using a different diffusion imaging protocol underlining their robustness.

FWf along the NBM lateral pathway was increased in both dementia and MCI groups, whereas a change in diffusivity metrics only became apparent at the dementia stage, indicating that excessive extracellular free water could be an early indicator of fiber degeneration and might precede changes in other diffusion metrics. However, longitudinal imaging studies will be needed to confirm this cross-sectional observation. FWf in the lateral NBM pathway was related to overall cognition, verbal fluency, and attentional performance. Additionally, we found elevated FWf in the lateral NBM pathway at baseline to be predictive of faster cognitive decline. This underscores the importance of the NBM cholinergic system for different aspects of cognitive function and confirms observations from studies in AD and PD that cholinergic changes are predictive of cognitive decline.[33,34]

In our previous study investigating the NBM pathways using a standard DTI model, we found changes in mean diffusivity that appeared to be similar to the changes in FWf that we saw here.[5] This agrees with similar observations from a previous study in AD and suggests that diffusion metrics in neurodegenerative disease are confounded by the presence of free water if this is not controlled for.[35] Both our present and previous analyses agree that the lateral NBM pathway is more severely affected in dementia than the medial pathway. However, the free water-corrected model revealed an increase in diffusivity in DLB and AD in the medial pathway that the single-tensor model failed to detect.[5] This suggests that free water correction can improve the sensitivity of DTI to detect neurodegenerative changes, aligning with previous findings in PD and AD.[20]

TABLE 3 Mean (standard deviation) and group comparison of diffusivity metrics from PPN and PPN-thalamus pathway.

			Controls	MCI-AD	MCI-LB	AD	DLB	Group differences	
A) PPN	FWf	Cohort 1	0.14 (0.04)	0.15 (0.05)	0.14 (0.04)	0.14 (0.04)	0.14 (0.04)	$F(4,230) = 1.0$, $P = .44$	
		Cohort 2	0.15 (0.05)	–	–	0.15 (0.05)	0.15 (0.05)	$F(2,97) = 0.07$, $P = .93$	
	FWc-AxD	Cohort 1	0.981 (0.04)	0.967 (0.05)	0.985 (0.05)	0.990 (0.04)	0.998 (0.05)	$F(4,230) = 1.6$, $P = .16$	
		Cohort 2	0.908 (0.054)	–	–	0.921 (0.073)	0.931 (0.064)	$F(2,97) = 0.89$, $P = .42$	
	FWc-MD	Cohort 1	0.590 (0.009)	0.591 (0.009)	0.590 (0.01)	0.593 (0.008)	0.593 (0.006)	$F(4,230) = 2.0$, $P = .09$	
		Cohort 2	0.598 (0.004)	–	–	0.598 (0.006)	0.598 (0.006)	$F(2,97) = 0.12$, $P = .89$	
B) PPN-thalamus pathway	FWf	Cohort 1	0.12 (0.02)	0.12 (0.02)	0.12 (0.02)	0.12 (0.02)	0.14 (0.03)	$F(4,230) = 3.7$, $P = .006$ P(HC,DLB) = 0.01 P(AD,DLB) = 0.009	HC, AD < DLB
		Cohort 2	0.13 (0.02)	–	–	0.15 (0.03)	0.16 (0.03)	$F(2,97) = 5.26$, $P = .007$ P(HC,DLB) = 0.005, P(AD,DLB) = 0.41	HC < DLB
	FWc-AxD	Cohort 1	0.899 (0.02)	0.90 (0.02)	0.913 (0.03)	0.902 (0.02)	0.909 (0.02)	$F(4,230) = 3.2$, $P = .015$ P(HC,MCI-LB) = 0.066 P(HC,DLB) = 0.052	HC < DLB
		Cohort 2	0.89 (0.03)	–	–	0.906 (0.04)	0.923 (0.028)	$F(2,97) = 6.09$, $P = .003$ P(HC,DLB) = 0.002	HC < DLB
	FWc-MD	Cohort 1	0.578 (0.01)	0.578 (0.009)	0.578 (0.01)	0.580 (0.01)	0.581 (0.01)	$F(4,230) = 0.86$, $P = .49$	
		Cohort 2	0.595 (0.005)	–	–	0.596 (0.005)	0.597 (0.006)	$F(2,97) = 0.44$, $P = .64$	

Note: Groups were compared by ANCOVAs including covariates for age, sex, and diffusivity metrics from a control mask. *P*-values from post hoc tests are Bonferroni-corrected for multiple comparisons. Axial and mean diffusivity values are multiplied by 1000.

All *P*-values from post hoc comparisons that are not shown are > 0.05.

Abbreviations: AD, Alzheimer's disease; DLB, dementia with Lewy bodies; FWc-AxD, free water-corrected axial diffusivity; FWc-MD, free water-corrected mean diffusivity; FWf, free water fraction; HC, healthy controls; MCI-AD, mild cognitive impairment due to Alzheimer's disease; MCI-LB, MCI with Lewy bodies; PPN, pedunculopontine nucleus.

TABLE 4 Beta values from multiple regression predicting cognitive scores (for baseline analysis) and annual change in cognitive scores (for longitudinal analysis) from free water fraction from NBM lateral and PPN-thalamus pathway including covariates for age, sex, and whole-brain metrics.

			N	FWf lateral NBM pathway	FWf PPN-thalamus pathway
MMSE	Cohort 1	Baseline	167	**$\beta = -0.32, P = .002$**	$\beta = 0.10, P = .20$
		Longitudinal	97	**$\beta = -0.34, P = .033$**	$\beta = 0.07, P = .54$
	Cohort 2	Baseline	68	$\beta = -0.27, P = .068$	$\beta = 0.03, P = .81$
		Longitudinal	44	$\beta = -0.36, P = .11$	$\beta = -0.08, P = .69$
CRT	Cohort 1	Baseline	155	$\beta = 0.19, P = .092$	$\beta = -0.02, P = .77$
		Longitudinal	74	**$\beta = 0.39, P = .031$**	$\beta = -0.17, P = .20$
	Cohort 2	Baseline	63	**$\beta = 0.32, P = .028$**	$\beta = 0.19, P = .15$
		Longitudinal	37	$\beta = 0.12, P = .60$	$\beta = 0.08, P = .69$
FAS	Cohort 1	Baseline	167	**$\beta = -0.25, P = .023$**	$\beta = -0.05, P = .58$
		Longitudinal	95	**$\beta = -0.38, P = .02$**	$\beta = 0.15, P = .24$
	Cohort 2	Baseline	66	**$\beta = -0.35, P = .011$**	$\beta = -0.19, P = .12$
		Longitudinal	42	$\beta = -0.28, P = .13$	$\beta = -0.02, P = .92$
UPDRS III motor scale	Cohort 1	Baseline	86	$\beta = 0.14, P = .41$	$\beta = 0.18, P = .15$
		Longitudinal	53	$\beta = 0.1, P = .64$	$\beta = 0.13, P = .41$
	Cohort 2	Baseline	34	$\beta = 0.33, P = .11$	$\beta = 0.35, P = .052$
		Longitudinal	14	$\beta = 0.35, P = .43$	$\beta = 0.50, P = .13$
CAF total	Cohort 1	Baseline	82	$\beta = 0.44, P = .008$*	$\beta = 0.02, P = .84$
		Longitudinal	44	$\beta = 0.01, P = .95$	$\beta = 0.21, P = .11$
	Cohort 2	Baseline	32	$\beta = -0.06, P = .78$	$\beta = 0.24, P = .25$
		Longitudinal	14	$\beta = -0.17, P = .78$	$\beta = 0.29, P = .64$
NPI hallucinations	Cohort 1	Baseline	82	$\beta = -0.07, P = .70$	**$\beta = 0.3, P = .017$**
		Longitudinal	48	$\beta = -0.01, P = .96$	$\beta = -0.11, P = .53$
	Cohort 2	Baseline	32	$\beta = 0.13, P = .58$	$\beta = -0.07, P = .73$
		Longitudinal	14	$\beta = 0.25, P = .43$	$\beta = 0.06, P = .81$

Abbreviations: CAF, Clinician Assessment of Fluctuations; CRT, choice reaction time; FAS, phonemic fluency test; FWf, free water fraction; MMSE, Mini-Mental State Examination; NBM, nucleus basalis of Meynert; NPI, Neuropsychiatric Inventory; PPN, pedunculopontine nucleus; UPDRS, Unified Parkinson's Disease Rating Scale.

*If no covariate for age is included: $\beta = 0.19, P = .21$.

FWf in the PPN-thalamus pathway was increased in DLB compared to controls, and—in contrast to the NBM pathways—this pathway was more severely affected in DLB than in AD. Furthermore, we found a correlation between FWf in the PPN-thalamus pathway and the NPI hallucination score and an increase in FWf in hallucinators versus non-hallucinators, thereby providing tentative evidence for an involvement of this pathway in visual hallucinations. Previous studies found an association between changes within the PPN and visual hallucinations in PD,[15,16] and several studies reported an involvement of the thalamus in the etiology of visual hallucinations in Lewy body disease.[36] We found that the integrity of the PPN-thalamus pathway was a stronger predictor of visual hallucination severity than microstructural properties of the PPN itself, indicating that, in particular, degeneration of the fiber tracts that provide cholinergic input to the thalamus might be an important contributor to the development of visual hallucinations. This decrease in cholinergic input might lead to alterations in thalamocortical rhythms, thereby disrupting the modulation of top-down and bottom-up attentional processes, increasing the likelihood of intrusions of incorrect perceptions.[37]

We found the PPN-thalamus pathway in AD to be significantly less affected than in DLB. Previous *post-mortem* studies found PPN cholinergic neurons to be relatively unaffected in AD,[38–41] and cholinergic imaging studies in the thalamus did not reveal differences between AD and controls.[18,42] Taken together, these findings indicate that the PPN cholinergic system is relatively spared, and the cholinergic input to the thalamus therefore remains intact in AD. We found no significant microstructural changes within the PPN itself in any group, which agrees with previous findings in PD.[20]

The multiple regression analysis suggests that the two parts of the cholinergic system appear relatively dissociated from each other in

terms of their involvement in different clinical symptoms. Furthermore, microstructural properties of the NBM and PPN pathways only moderately correlated with each other, indicating that the two parts of the cholinergic system are not necessarily similarly affected in each patient. Thus, changes in different parts of the cholinergic system can occur independently of each other and can have different clinical consequences.

The bi-tensor DTI model used here is advantageous compared to a single-tensor model in two ways. First, the adjustment of diffusion metrics for the presence of free water can improve sensitivity to disease-related changes,[20] an observation that was confirmed here. Additionally, this model provides a separate biomarker for the fraction of free water in each voxel. The exact biological underpinnings of this measure are still under investigation, but there is growing evidence that it might be related to inflammation,[22] with evidence from preclinical studies[43] and studies linking free water in the brain to peripheral markers of inflammation[23] and MR spectroscopy measures of immune function.[44] The results of the present study are therefore relevant in the context of a growing interest in neuroinflammation as a potential contributor in DLB and AD.[45] However, free water imaging is unable to distinguish between inflammation and increases in extracellular space due to atrophy. More direct in vivo measures of neuroinflammation using new PET ligands could be used to investigate this further.

5 | LIMITATIONS

The majority of patients were taking cholinesterase inhibitors, which might have influenced NBM degeneration.[46] The prescription rates in our study sample reflect local prescription practices following recent guidelines,[47] and we found no differences in diffusivity metrics based on the use of cholinesterase inhibitors.

Another potential limitation is the lack of AD biomarkers in this study since it has been shown that the integrity of the NBM pathways is related to both amyloid and tau pathology in patients along the AD continuum.[48] Studying the influence of AD copathology on cholinergic changes in DLB will be an interesting avenue for future research.

The PPN is a small structure that contains glutamatergic and GABAergic neurons.[7] We can therefore not rule out the possibility that the PPN region that we analyzed contained some non-cholinergic neurons. However, the PPN-thalamic projections have been shown to be predominantly cholinergic.[49] The analyzed NBM tracts were similar to previously identified tracts from an immunohistochemistry study in which their cholinergic nature was confirmed.[50]

Estimating FWf from single-shell diffusion data requires some regularizations, and it is difficult to be certain that diffusion imaging is measuring the same pathological process in the NBM and the PPN as these structures are surrounded by different anatomy. More advanced multishell acquisitions are needed to test the reliability of these methods. Additionally, the low resolution and number of diffusion directions in Cohort 2 might have affected the estimation of diffusivity measures.

6 | CONCLUSION

This study provides further insight into changes within the complex architecture of the cholinergic system in AD and DLB, suggesting that the NBM and its cholinergic projections to the cortex degenerate early in both conditions affecting various aspects of cognitive function. In contrast, the cholinergic input to the thalamus that is provided by the PPN appears to be more selectively impaired in DLB. Cholinergic medication is one of the mainstays of symptomatic treatment in AD and DLB, and both PPN and NBM have been investigated as targets for deep brain stimulation,[47] highlighting the clinical relevance of these findings.

ACKNOWLEDGMENTS

We would like to thank colleagues at Hospital Israelita Albert Einstein, Instituto do Cérebro (São Paulo, Brazil), for sharing the PPN mask generated in Alho et al. (2017) and Andrew Blamire (Newcastle University Translational and Clinical Research Institute) for data sharing. This research was funded by Alzheimer's Research UK (ARUK-PG2015-13), a Wellcome Trust Intermediate Clinical Fellowship (WT088441MA) to JPT, and the Sir Jules Thorn Charitable Trust. The research was supported by the NIHR Newcastle Biomedical Research Centre (grants BH120812 and BH120878) and Northumberland Tyne and Wear NHS Foundation Trust. G.E. Healthcare provided the FP-CIT radioligand for diagnostic assessment of MCI participants in this investigator-led study. PCD was supported by the Medical Research Council (grant MR/W000229/1). LA was supported by the National Institute for Health Research Applied Research Collaboration South West Peninsula. The views expressed in this publication are those of the author(s) and do not necessarily reflect the views of the National Institute for Health Research or the Department of Health and Social Care.

CONFLICT OF INTEREST STATEMENT

Author disclosures are available in the supporting information.

CONSENT STATEMENT

Written informed consent was obtained from all participants in this study.

ORCID

Julia Schumacher https://orcid.org/0000-0001-7323-4789

REFERENCES

1. Bohnen NI, Grothe MJ, Ray NJ, Müller MLTM, Teipel SJ. Recent advances in cholinergic imaging and cognitive decline—revisiting the cholinergic hypothesis of dementia. *Curr Geriatr Reports*. 2018;7:1-11. doi:10.1007/s13670-018-0234-4
2. Mesulam M-M. Cholinergic circuitry of the human nucleus basalis and its fate in Alzheimer's disease. *J Comp Neurol*. 2013;521:4124-4144. doi:10.1002/cne.23415
3. Teipel SJ, Cavedo E, Grothe MJ, et al. Predictors of cognitive decline and treatment response in a clinical trial on suspected prodromal Alzheimer's disease. *Neuropharmacology*. 2016;108:128-135. doi:10.1016/j.neuropharm.2016.02.005

4. Schumacher J, Taylor J, Hamilton CA, et al. In vivo nucleus basalis of Meynert degeneration in mild cognitive impairment with Lewy bodies. *NeuroImage Clin*. 2021;30:102604. doi:10.1016/j.nicl.2021.102604
5. Schumacher J, Ray NJ, Hamilton CA, et al. Cholinergic white matter pathways in dementia with Lewy bodies and Alzheimer's disease. *Brain*. 2022;145:1773-1784. doi:10.1093/brain/awab372
6. Aravamuthan BR, Muthusamy KA, Stein JF, Aziz TZ, Johansen-Berg H. Topography of cortical and subcortical connections of the human pedunculopontine and subthalamic nuclei. *Neuroimage*. 2007;37:694-705. doi:10.1016/j.neuroimage.2007.05.050
7. Mena-Segovia J, Bolam JP. Rethinking the pedunculopontine nucleus: from cellular organization to function. *Neuron*. 2017;94:7-18. doi:10.1016/j.neuron.2017.02.027
8. Bohnen NI, Muller MLTM, Koeppe RA, et al. History of falls in Parkinson disease is associated with reduced cholinergic activity. *Neurology*. 2009;73:1670-1676. doi:10.1212/WNL.0b013e3181c1ded6
9. Gut NK, Mena-Segovia J. Dichotomy between motor and cognitive functions of midbrain cholinergic neurons. *Neurobiol Dis*. 2019;128:59-66. doi:10.1016/j.nbd.2018.09.008
10. Marsel MesulamM, Geula C, Bothwell MA, Hersh LB. Human reticular formation: cholinergic neurons of the pedunculopontine and laterodorsal tegmental nuclei and some cytochemical comparisons to forebrain cholinergic neurons. *J Comp Neurol*. 1989;283:611-633. doi:10.1002/cne.902830414
11. Mesulam M-M, Mufson EJ, Wainer BH, Levey AI. Central cholinergic pathways in the rat: an overview based on an alternative nomenclature (Ch1–Ch6). *Neuroscience*. 1983;10:1185-1201. doi:10.1016/0306-4522(83)90108-2
12. Vitale F, Capozzo A, Mazzone P, Scarnati E. Neurophysiology of the pedunculopontine tegmental nucleus. *Neurobiol Dis*. 2019;128:19-30. doi:10.1016/j.nbd.2018.03.004
13. Schmeichel AM, Buchhalter LC, Low PA, et al. Mesopontine cholinergic neuron involvement in Lewy body dementia and multiple system atrophy. *Neurology*. 2008;70:368-373. doi:10.1212/01.wnl.0000298691.71637.96
14. Seidel K, Mahlke J, Siswanto S, et al. The brainstem pathologies of Parkinson's disease and dementia with lewy bodies. *Brain Pathol*. 2015;25:121-135. doi:10.1111/bpa.12168
15. Hepp DH, Ruiter AM, Galis Y, et al. Pedunculopontine cholinergic cell loss in hallucinating Parkinson disease patients but not in dementia with lewy bodies patients. *J Neuropathol Exp Neurol*. 2013;72:1162-1170. doi:10.1097/NEN.0000000000000014
16. Janzen J, van 't Ent D, Lemstra AW, Berendse HW, Barkhof F, Foncke EMJ. The pedunculopontine nucleus is related to visual hallucinations in Parkinson's disease: preliminary results of a voxel-based morphometry study. *J Neurol*. 2012;259:147-154. doi:10.1007/s00415-011-6149-z
17. Kanel P, Müller MLTM, van der Zee S, et al. Topography of cholinergic changes in dementia with lewy bodies and key neural network hubs. *J Neuropsychiatry Clin Neurosci*. 2020;32:370-375. doi:10.1176/appi.neuropsych.19070165
18. Kotagal V, Müller MLTM, Kaufer DI, Koeppe RA, Bohnen NI. Thalamic cholinergic innervation is spared in Alzheimer disease compared to parkinsonian disorders. *Neurosci Lett*. 2012;514:169-172. doi:10.1016/j.neulet.2012.02.083
19. Alho ATDL, Hamani C, Alho EJL, et al. Magnetic resonance diffusion tensor imaging for the pedunculopontine nucleus: proof of concept and histological correlation. *Brain Struct Funct*. 2017;222:2547-2558. doi:10.1007/s00429-016-1356-0
20. Ray NJ, Lawson RA, Martin SL, et al. Free-water imaging of the cholinergic basal forebrain and pedunculopontine nucleus in Parkinson's disease. *Brain*. 2022;146:1053-1064. doi:10.1093/brain/awac127
21. Pasternak O, Sochen N, Gur Y, Intrator N, Assaf Y. Free water elimination and mapping from diffusion MRI. *Magn Reson Med*. 2009;62:717-730. doi:10.1002/mrm.22055
22. Oestreich LKL, O'Sullivan MJ. Transdiagnostic in vivo magnetic resonance imaging markers of neuroinflammation. *Biol Psychiatry Cogn Neurosci Neuroimaging*. 2022:1-21. doi:10.1016/j.bpsc.2022.01.003
23. Di Biase MA, Zalesky A, Cetin-Karayumak S, et al. Large-scale evidence for an association between peripheral inflammation and white matter free water in schizophrenia and healthy individuals. *Schizophr Bull*. 2021;47:542-551. doi:10.1093/schbul/sbaa134
24. Nemy M, Cedres N, Grothe MJ, et al. Cholinergic white matter pathways make a stronger contribution to attention and memory in normal aging than cerebrovascular health and nucleus basalis of Meynert. *Neuroimage*. 2020;211:116607. doi:10.1016/j.neuroimage.2020.116607
25. Donaghy PC, Firbank M, Petrides G, et al. Diffusion imaging in dementia with Lewy bodies: associations with amyloid burden, atrophy, vascular factors and clinical features. *Parkinsonism Relat Disord*. 2020;78:109-115. doi:10.1016/j.parkreldis.2020.07.025
26. Watson R, O'Brien JT, Barber R, Blamire AM. Patterns of gray matter atrophy in dementia with Lewy bodies: a voxel-based morphometry study. *Int Psychogeriatrics*. 2012;24:532-540. doi:10.1017/S1041610211002171
27. McKeith IG, Boeve BF, Dickson DW, et al. Diagnosis and management of dementia with Lewy bodies Fourth consensus report of the DLB Consortium. *Neurology*. 2017;0:1-13.
28. McKhann GM, Knopman DS, Chertkow H, et al. The diagnosis of dementia due to Alzheimer's disease: recommendations from the National Institute on Aging-Alzheimer's Association workgroups on diagnostic guidelines for Alzheimer's disease. Alzheimer's. *Dement*. 2011;7:263-269. doi:10.1016/j.jalz.2011.03.005
29. McKeith IG, Ferman TJ, Thomas AJ, et al. Research criteria for the diagnosis of prodromal dementia with Lewy bodies. *Neurology*. 2020.
30. Albert MS, DeKosky ST, Dickson D, et al. The diagnosis of mild cognitive impairment due to Alzheimer's disease: recommendations from the National Institute on Aging-Alzheimer's Association workgroups on diagnostic guidelines for Alzheimer's disease. Alzheimer's. *Dement*. 2011;7:270-279. doi:10.1016/j.jalz.2011.03.008
31. Hamilton CA, Matthews FE, Donaghy PC, et al. Cognitive decline in mild cognitive impairment with lewy bodies or Alzheimer disease: a prospective cohort study. *Am J Geriatr Psychiatry*. 2021;29:272-284. doi:10.1016/j.jagp.2020.07.018
32. Kilimann I, Grothe M, Heinsen H, et al. Subregional basal forebrain atrophy in Alzheimer's disease: a multicenter study. *J Alzheimer's Dis*. 2014;40:687-700. doi:10.3233/JAD-132345
33. Ray NJ, Bradburn S, Murgatroyd C, et al. In vivo cholinergic basal forebrain atrophy predicts cognitive decline in de novo Parkinson's disease. *Brain*. 2018;141:165-176. doi:10.1093/brain/awx310
34. Brueggen K, Dyrba M, Barkhof F, et al. Basal forebrain and hippocampus as predictors of conversion to Alzheimer's disease in patients with mild cognitive impairment – a multicenter DTI and volumetry study. *J Alzheimer's Dis*. 2015;48:197-204. doi:10.3233/JAD-150063
35. Bergamino M, Walsh RR, Stokes AM. Free-water diffusion tensor imaging improves the accuracy and sensitivity of white matter analysis in Alzheimer's disease. *Sci Rep*. 2021;11:6990. doi:10.1038/s41598-021-86505-7
36. Matar E, Brooks D, Lewis SJG, Halliday GM. Limbic thalamus atrophy is associated with visual hallucinations in Lewy body disorders. *Neurobiol Aging*. 2022;112:122-128. doi:10.1016/j.neurobiolaging.2022.01.001
37. Collerton D, Perry EK, McKeith I. Why people see things that are not there: a novel perception and attention deficit model for recurrent complex visual hallucinations. *Behav Brain Sci*. 2005;28:737-757. doi:10.1017/S0140525%D7;05000130. discussion 757-94.
38. Jellinger K. The pedunculopontine nucleus in Parkinson's disease, progressive supranuclear palsy and Alzheimer's disease. *J Neurol Neurosurg Psychiatry*. 1988;51:540-543. doi:10.1136/jnnp.51.4.540
39. Dugger BN, Murray ME, Boeve BF, et al. Neuropathological analysis of brainstem cholinergic and catecholaminergic nuclei in relation to

rapid eye movement (REM) sleep behaviour disorder. *Neuropathol Appl Neurobiol*. 2012;38:142-152. doi:10.1111/j.1365-2990.2011.01203.x

40. Woolf NJ, Jacobs RW, Butcher LL. The pontomesencephalotegmental cholinergic system does not degenerate in Alzheimer's disease. *Neurosci Lett*. 1989;96:277-282. doi:10.1016/0304-3940(89)90391-1
41. Brandel J-P, Hirsch EC, Malessa S, Duyckaerts C, Cervera P, Agid Y. Differential vulnerability of cholinergic projections to the mediodorsal nucleus of the thalamus in senile dementia of Alzheimer type and progressive supranuclear palsy. *Neuroscience*. 1991;41:25-31. doi:10.1016/0306-4522(91)90197-V
42. Nejad-Davarani S, Koeppe RA, Albin RL, Frey KA, Müller MLTM, Bohnen NI. Quantification of brain cholinergic denervation in dementia with Lewy bodies using PET imaging with [18F]-FEOBV. *Mol Psychiatry*. 2019;24:322-327. doi:10.1038/s41380-018-0130-5
43. Di Biase MA, Katabi G, Piontkewitz Y, Cetin-Karayumak S, Weiner I, Pasternak O. Increased extracellular free-water in adult male rats following in utero exposure to maternal immune activation. *Brain Behav Immun*. 2020;83:283-287. doi:10.1016/j.bbi.2019.09.010
44. Lesh TA, Maddock RJ, Howell A, et al. Extracellular free water and glutathione in first-episode psychosis—a multimodal investigation of an inflammatory model for psychosis. *Mol Psychiatry*. 2021;26:761-771. doi:10.1038/s41380-019-0428-y
45. Amin J, Erskine D, Donaghy PC, et al. Inflammation in dementia with Lewy bodies. *Neurobiol Dis*. 2022;168:105698. doi:10.1016/j.nbd.2022.105698
46. Cavedo E, Grothe MJ, Colliot O, et al. Reduced basal forebrain atrophy progression in a randomized Donepezil trial in prodromal Alzheimer's disease. *Sci Rep*. 2017;7:11706. doi:10.1038/s41598-017-09780-3
47. Taylor J-P, McKeith IG, Burn DJ, et al. New evidence on the management of Lewy body dementia. *Lancet Neurol*. 2020;19:157-169. doi:10.1016/S1474-4422(19)30153-X
48. Nemy M, Dyrba M, Brosseron F, et al. Cholinergic white matter pathways along the Alzheimer's disease continuum. *Brain*. 2022. doi:10.1093/brain/awac385
49. Sofroniew MV, Priestley JV, Consolazione A, Eckenstein F, Cuello AC. Cholinergic projections from the midbrain and pons to the thalamus in the rat, identified by combined retrograde tracing and choline acetyltransferase immunohistochemistry. *Brain Res*. 1985;329:213-223. doi:10.1016/0006-8993(85)90527-X
50. Selden N, Gitelman DR, Salamon-Murayama N, Parrish TB, Mesulam M-M. Trajectories of cholinergic pathways within the cerebral hemispheres of the human brain. *Brain*. 1998;121:2249-2257. doi:10.1093/brain/121.12.2249

SUPPORTING INFORMATION

Additional supporting information can be found online in the Supporting Information section at the end of this article.

How to cite this article: Schumacher J, Ray NJ, Hamilton CA, et al. Free water imaging of the cholinergic system in dementia with Lewy bodies and Alzheimer's disease. *Alzheimer's Dement*. 2023;1-15. https://doi.org/10.1002/alz.13034